Large Lenses of Highly Saline Mediterranean Water

LAURENCE ARMI

Scripps Institution of Oceanography, La Jolla, CA 92093

WALTER ZENK

Institut für Meereskunde an der Universität Kiel, 2300 Kiel 1, Germany

(Manuscript received 1 May 1984, in final form 27 June 1984)

ABSTRACT

Isolated compact anticyclonic eddies or salt lenses were found in the Canary Basin. Hydrographic surveys of three such lenses show large anomalies of salinity and temperature (~0.8, 2.5°C). They are centered at ~1100 m, have a vertical extent of up to 900 m and radii of ~50 km. Current meter records indicate anticyclonic velocities up to 29 cm s^{-1}. Fine structure with vertical scales of ~20 m and less, possibly due to intrusive decay, appears at the outer edges of the lenses whereas the centers are free of such structure. The probability of finding a salt lens at any station in the Canary Basin is fairly high (~0.08).

1. Introduction

Lens-shaped structures or isolated compact eddies found at several locations in the Canary Basin are reported here. An example of a profile through such a feature found at 33°0'N, 20°28'W is shown in Fig. 1. The lens station (104) is contrasted with a typical background station (85) ~ 85 km away. The anomalies of salinity and temperature are large (~0.8, 25°C)[1] as are their vertical extent (~900 m).

A similar anomaly was found at 26°32'N, 29°06'W (~1000 km to the southwest) by Armi and Stommel (1983, Fig. 7.8). Although it is impossible to determine the shapes of these features from single stations, the hydrographic surveys reported here found them to be nearly lens-shaped. They will simply be called lenses, knowing well that the detailed structure may not be exactly that of a lens. The three lenses found were all double-convex and rotating anticyclonically. A pinched or double-concave structure rotating cyclonically might exist but was not noticed in the region surveyed.

Lens-shaped structures have been found in other parts of the ocean before. Without attempting to be comprehensive, we are aware of a study of similar, although somewhat less anomalous features (a.k.a. Meddies) in the Western North Atlantic reported by McDowell and Rossby (1978), Rossby *et al.* (1983), and Riser *et al.* (1984). A comprehensive survey of sub-mesoscale, coherent vortices in the ocean has recently been completed by McWilliams (1984). Armi (1978) and Armi and D'Asaro (1980) found similar flow structures in the abyssal ocean.

Although the lens structures reported here have an unambiguous Mediterranean Water source based on their hydrography, the actual formation mechanism is not completely clear. A small deep eddy was found off Cape St. Vincent by Swallow (1969) and a tantalizing report of large cells of Mediterranean Water in the Madeira–Canaries Region was given by Piip (1969). A preliminary report of the hydrographic data presented here was made by Armi (1981).

2. Hydrographic surveys

The surveys described below were conducted in June 1981 as part of Leg III of the Transient Tracers in the Oceans (TTO) North Atlantic Study aboard the R.V. *Knorr*. Station locations and the three lenses surveyed are shown in Figs. 2 and 3; lenses are numbered sequentially in order of discovery. This broad-scale survey was designed to study the distribution of salinity, nutrients, and transient tracers associated with the Mediterranean Water and at the same time optimize chances of finding another anomalously salty lens as suggested by the isolated station to the southwest of Armi and Stommel (1983). A preliminary hydrographic data report is available from the SIO Physical and Chemical Oceanographic Data Facility (1981).

A salinity section from SE to NW through salt lens 3 is shown in Fig. 4. The positions of the stations chosen for this section are shown in Fig. 3. This section clearly shows the vertical and horizontal

[1] The international equation of state and practical salinity standard have been used to make all calculations (JPOTS, 1980). Salinity is now nondimensional.

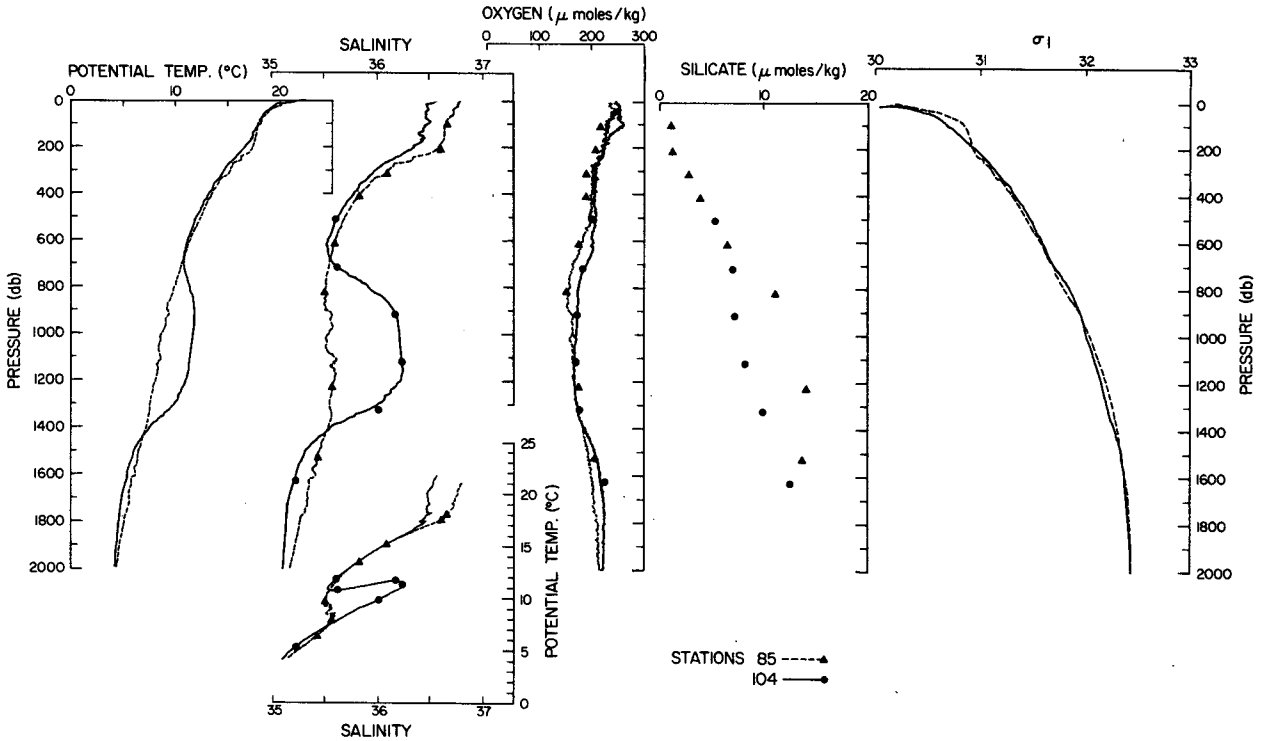

FIG. 1. Comparison profiles of potential temperature, salinity, oxygen, silicate and σ_1 vs. pressure, and potential temperature vs. salinity for a salt lens station (station 104, 33°0'N, 21°28'W) and a nearby background station 85 km away (station 85, 32°15'N, 21°17'W). Continuous profiles are from downcasts of the profiler whereas the discrete data are from bottles closed on the upcast.

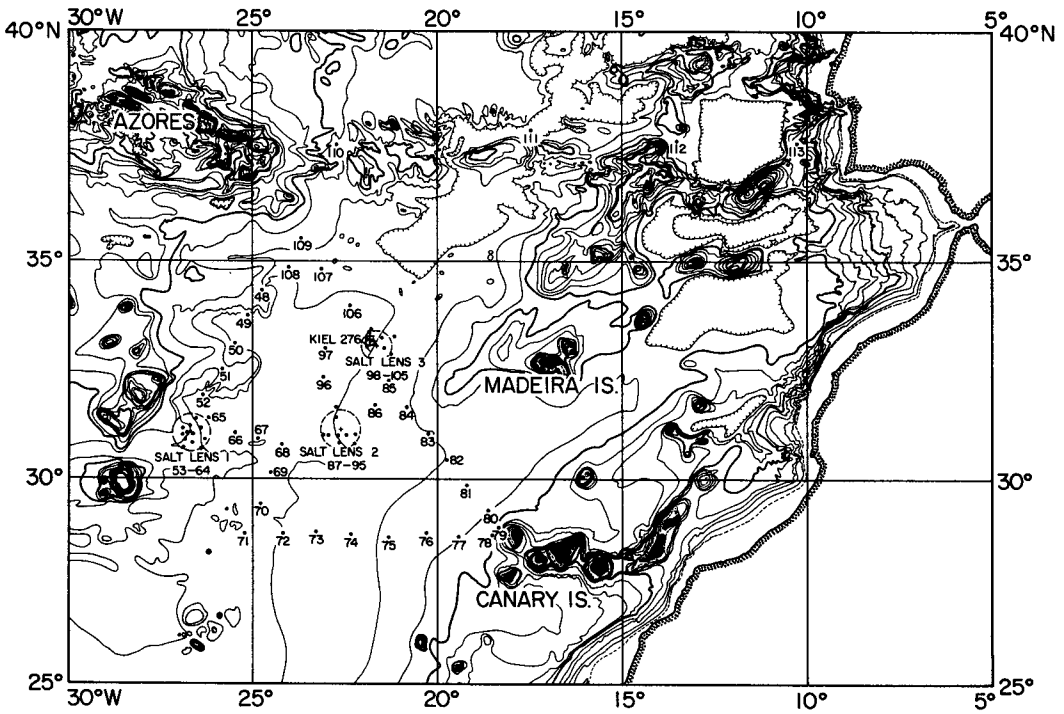

FIG. 2. Large-scale topography (Uchupi, 1971) and station positions in the Canary Basin. Isobaths are shown at 400 m intervals.

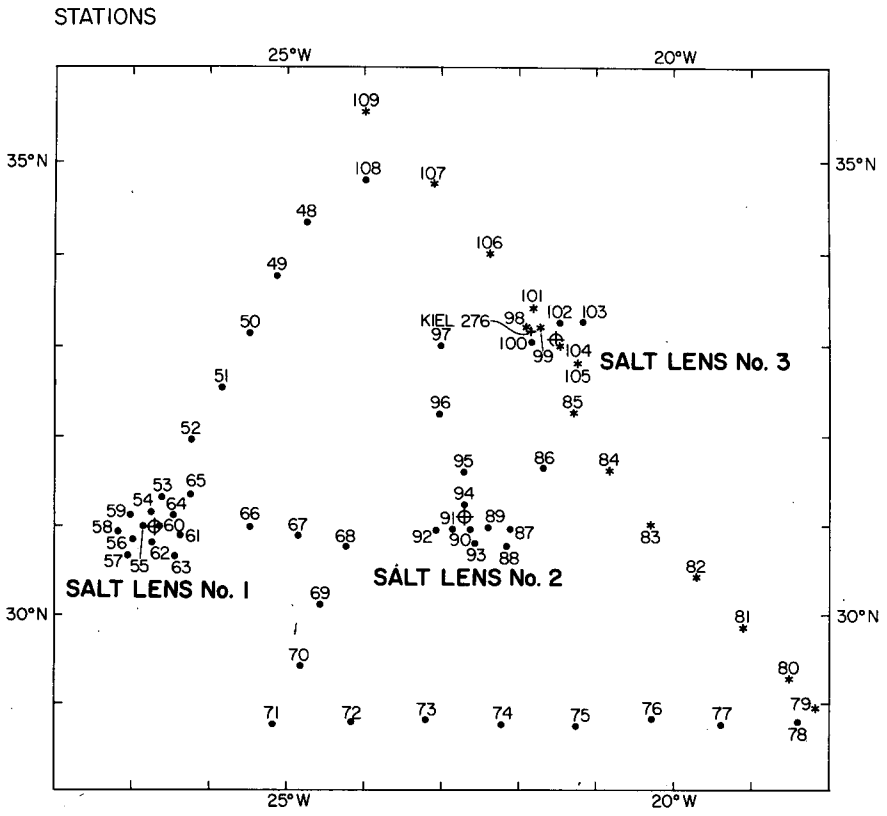

FIG. 3. Detailed station map. Stations marked with an asterisk are used in the salinity section (Fig. 4). Approximate lens centers are shown as is the position of Kiel mooring 276.

extent of the salt lens (stations 98, 99, 101, 104, 105). A fourth lens may be located to the NW of this lens (station 106); however, insufficient ship time remained to survey it.

The times and locations of beginning and ending stations for each of the lens surveys are shown in Table 1. A maximum of 48 h was spent on the hydrographic surveying of each lens. It will be later seen from moored-current-meter data that advection velocities associated with the entire lens structure (not velocities within the lens) are O(~5 cm s^{-1}). Hence the time required to survey the lenses results in errors of order 10 km from the beginning to end of each survey due to lack of true synopticity.

Although only a limited number of stations was taken in each of three lenses, considerable information regarding their dynamics and distribution of properties can be inferred if each lens is assumed to be circularly symmetric. The distribution of maximum salinity at the salinity midwater maximum (~1100 db) was fitted using a linear regression to a paraboloid. This results in four parameters found by the fit: position

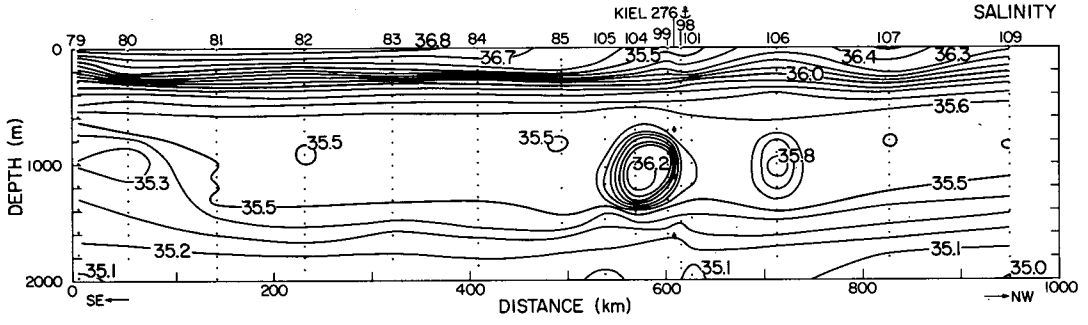

FIG. 4. Salinity section from SE (approximately 29°N, 18°W) to NW (approximately 35°30'N, 24°W) through salt lens 3. The position and configuration of current meters at Kiel mooring 276 are also shown.

TABLE 1. Beginning and ending stations of individual lens surveys.

Lens	Station	Date	GMT	Position
1	53	28 May 81	1633	31°19'N, 26°37'W
	65	30 May 81	1548	31°21'N, 26°14'W
2	87	7 June 81	2042	30°58'N, 22°07'W
	95	9 June 81	0414	31°36'N, 22°42'W
3	98	10 June 81	0528	33°13'N, 21°55'W
	105	11 June 81	1709	32°49'N, 21°15'W

of the lens center (x, y), salinity at the center, and the radius of the lens. The maximum salinity distribution found is contoured in Figs. 5–7.

Using the radii from the regression shown in Figs. 5–7, data for the fitted maximum salinity, as well as maximum potential temperature, lens thickness (defined by the depth range over which the salinity exceeded 35.7) and dynamic height (1000/1900 db) are shown in Figs. 8–10. Stations considered near but outside the lenses are shown in Fig. 8 but indicated by lighter points. (These stations were also excluded from the regression.) Positional errors shown are due to the error in lens center position from each regression fit.

The paraboloid of best fit to the maximum salinity appears to represent the distributions of salinity and potential temperature in the lenses, except near the lens centers. Figures 8–10 suggest the distribution is nearly homogeneous in the lens centers out to a radius of ~25 km. This will also be seen in the profiles of Figs. 11–13.

The velocity gradient given by the dynamic height (1000/1900 db) is of order 20–24 cm s^{-1} between 20 and 40 km. The third lens was surveyed when velocities near its edge were being recorded by a current meter mooring (Kiel 276). Discussion of these results can be found in the next section.

Profiles of salinity, potential temperature and σ_1 are shown in Figs. 11–13. These profiles are from a Neil Brown CTD at ~1 db vertical resolution. The position of each station on the latitude–longitude

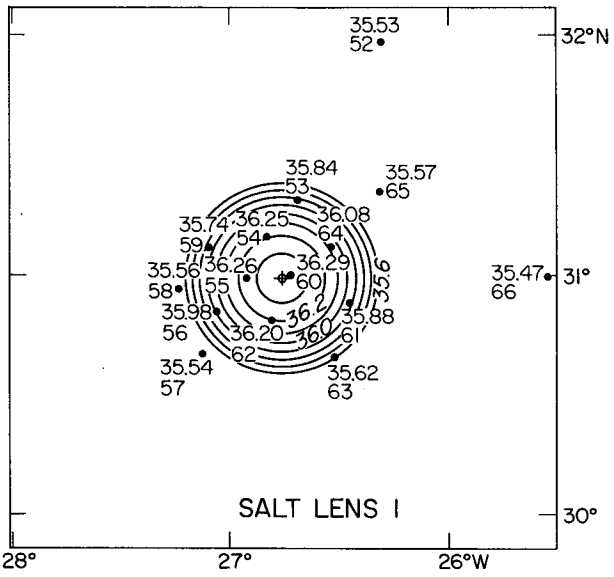

FIG. 5. The distribution of maximum salinity at the salinity midwater maximum from a linear regression to a paraboloidal distribution. Maximum salinities and station numbers are also shown. Salt lens 1.

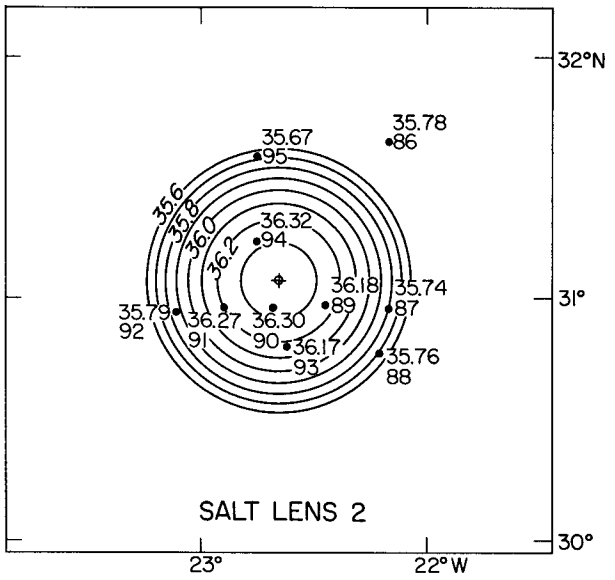

FIG. 6. As in Fig. 5 but for salt lens 2.

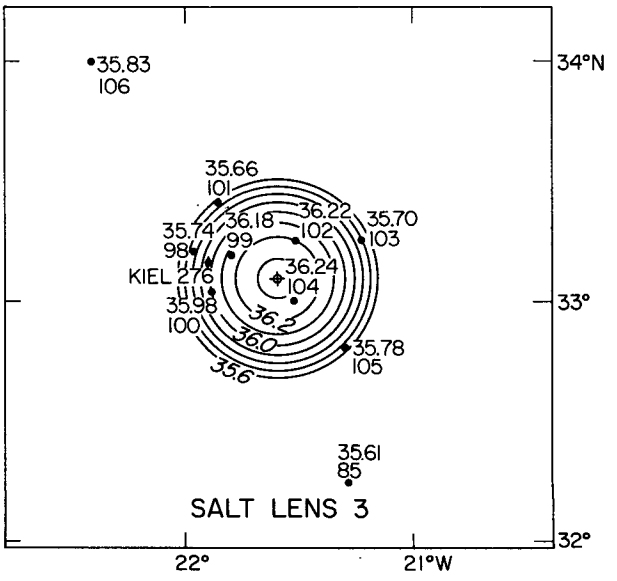

FIG. 7. As in Fig. 5 but for salt lens 3.

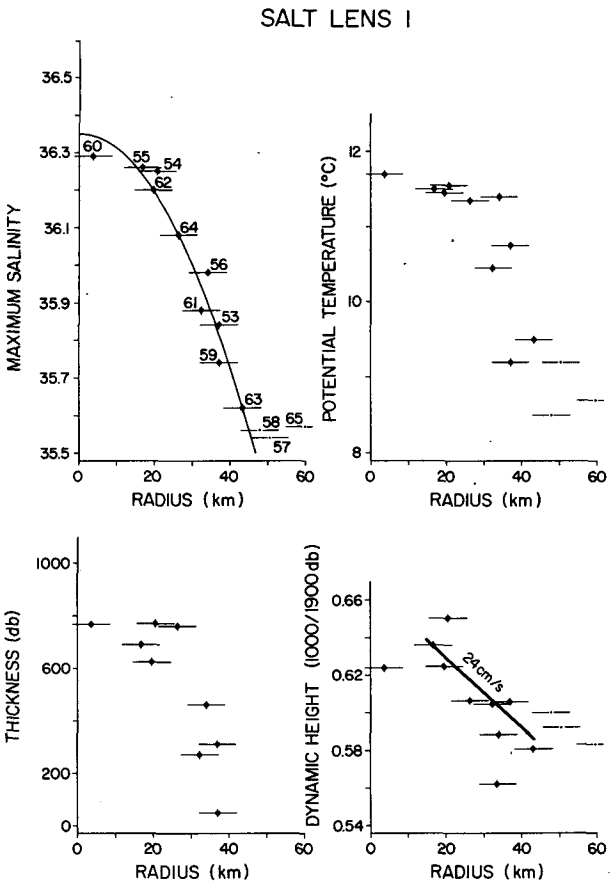

FIG. 8. Radial distributions of maximum salinity and potential temperature (at the salinity midwater maximum), lens thickness (defined by salinity > 35.7) and relative (1000/1900 db) dynamic height (dyn m). Stations considered outside the lens are shown as lighter points. Salt lens 1.

map is indicated by a cross. Scales for the profiles are only shown once and are the same for all the profiles. In the lens center the maximum salinity is as high as 36.3 in a field of typical maximum salinities of 35.5–35.6. An anomaly of 0.8 in salinity and 2.5°C in potential temperature is seen at the center of the lenses.

Near the lens centers, the profiles are relatively smooth with little evidence of fine structure. However, scanning across the lenses, for example at latitude 31°N in Fig. 11, one sees that profiles taken towards the edges of the lenses exhibit considerable fine structure with vertical scales of ~20 m and less. This fine structure is possibly due to intrusive decay of the lenses at their edges. At the station spacing dictated by the equipment and time available, this intrusive structure is completely undersampled. Further, it is interesting to note that the step-like structures beneath the Mediterranean core layer only can be found at the peripheral stations. Excellent examples are stations 101 and 103 in Fig. 13. This pronounced form of fine structure may be indicative of salt fingering as discussed by Turner (1973) and reported earlier for a site 1000 km east of lens 3 by Siedler and Zenk (1973). It may also be indicative of a double-diffusive instability of momentum and mass as discussed by McIntyre (1970).

The distribution of dynamic heights at 1000 db with respect to 1900 db shows an anticyclonic motion with a velocity of ~22 cm s^{-1} at radii between 30 and 45 km. The assumption of circular symmetry only allows us to estimate the rotational component of the velocity. The weak gradients of dynamic height near the lens center, at a radius less than 30 km, suggest a more slowly rotating center. Dynamic height gradients alone may not, however, be adequate for velocity determination near the lens center where centripetal accelerations may also become important.

3. Eulerian observations

In 1977 the Institut für Meereskunde Kiel (IFM) started a moderate moored current meter program in the central Canary Basin as part of the international North-Eastern Atlantic Dynamic Studies (NEADS). With interruptions, this mooring site was maintained

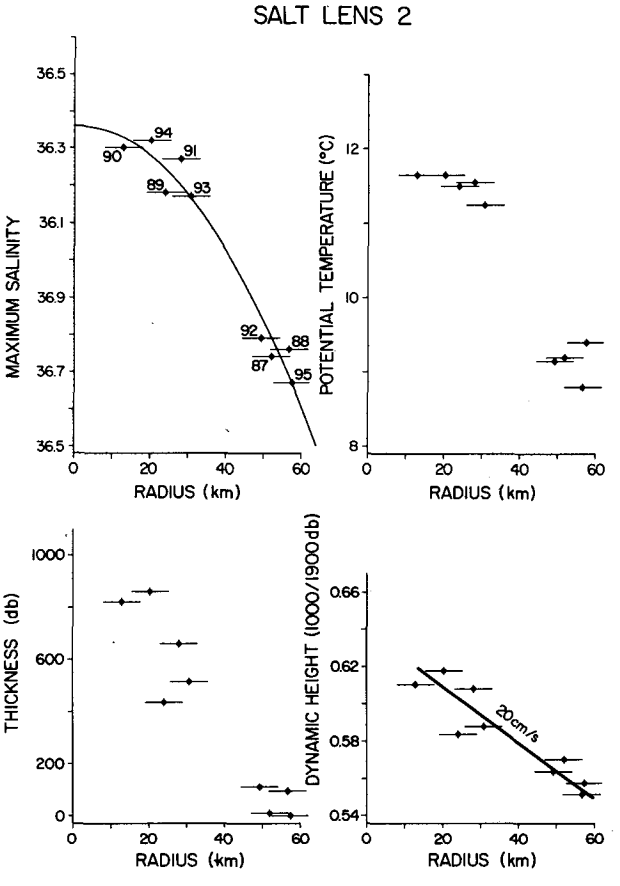

FIG. 9. As in Fig. 8 but for salt lens 2.

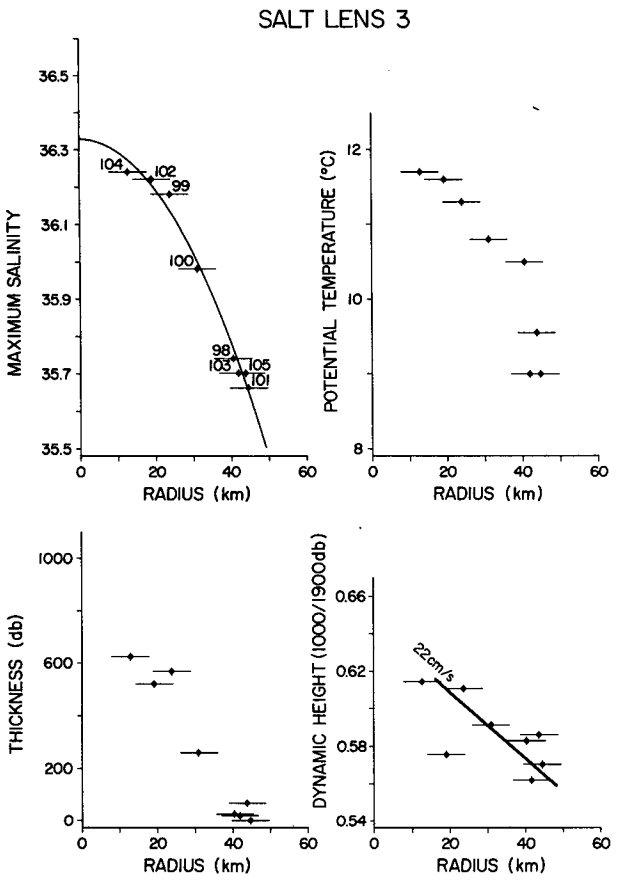

FIG. 10. As in Fig. 8 but for salt lens 3.

until October 1980 (Müller, 1981) and has since then been continued with extended instrumentation under the long-term research program "Warmwassersphäre des Atlantik." Fortunately, one salt lens passed the KIEL 276 mooring while simultaneous hydrographic detail observations were conducted aboard R.V. *Knorr*. The mooring was situated at 33°9.9'N, 21°50.9'W (Figs. 2 and 3) and was instrumented besides other levels at 703, 1004, 1106 and 1608 m (Fig. 4). The sampling interval of the Aanderaa current meters, exclusively used here, was 1 hour. A complete data report from mooring 276 and related other Warmwassersphäre moorings and from simultaneous XBT sections is available (Müller and Zenk, 1983). We will restrict ourselves here to a subset of the moored data from 24 May through 21 June 1981. This time span includes the *Knorr* visit to the site.

Figure 14 shows an unfiltered time series of the recorded velocity vectors (in polar coordinates), the corresponding temperature data, and for the 703 m instrument also, the pressure record. The stippled region of Fig. 14 (10 and 11 June 1981) is the time frame of the R.V. *Knorr* observations. Table 2 summarizes the basic statistical parameters of the original time series shown in Fig. 14. Although the mean and standard deviation statistics are shown, their interpretation must be done with caution. Later (cf. Fig. 18) it will be seen that these statistics are almost completely dominated by the occurrence of salt lenses!

The approach of lens 3 can be recognized at 1004 and 1106 m (Fig. 14) by a slow increase of tempera-

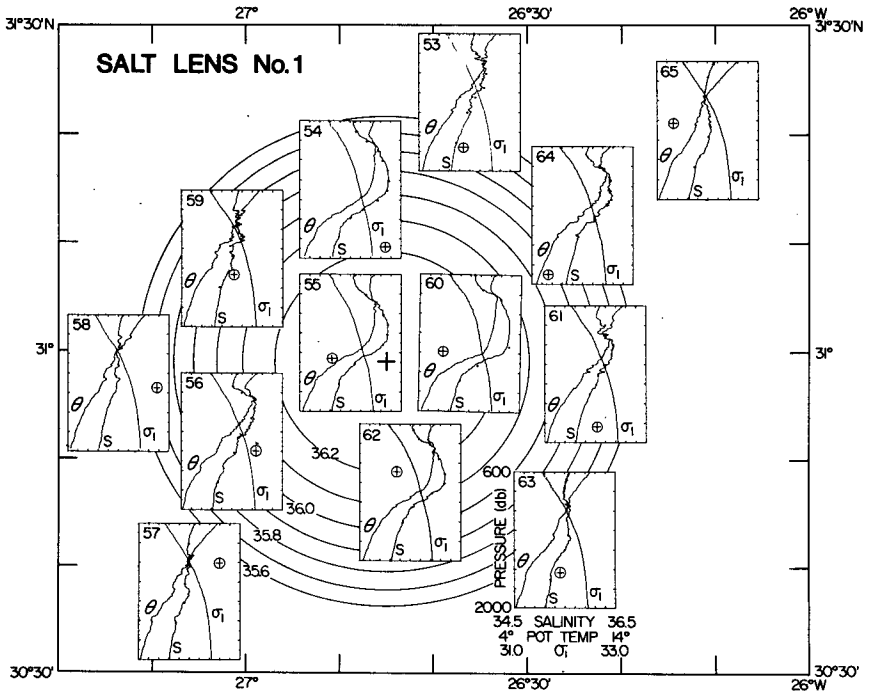

FIG. 11. Detailed station profiles of salinity, potential temperature (θ) and density (σ_1). The position of each station is indicated on the fitted distribution of maximum salinity. Salt lens 1.

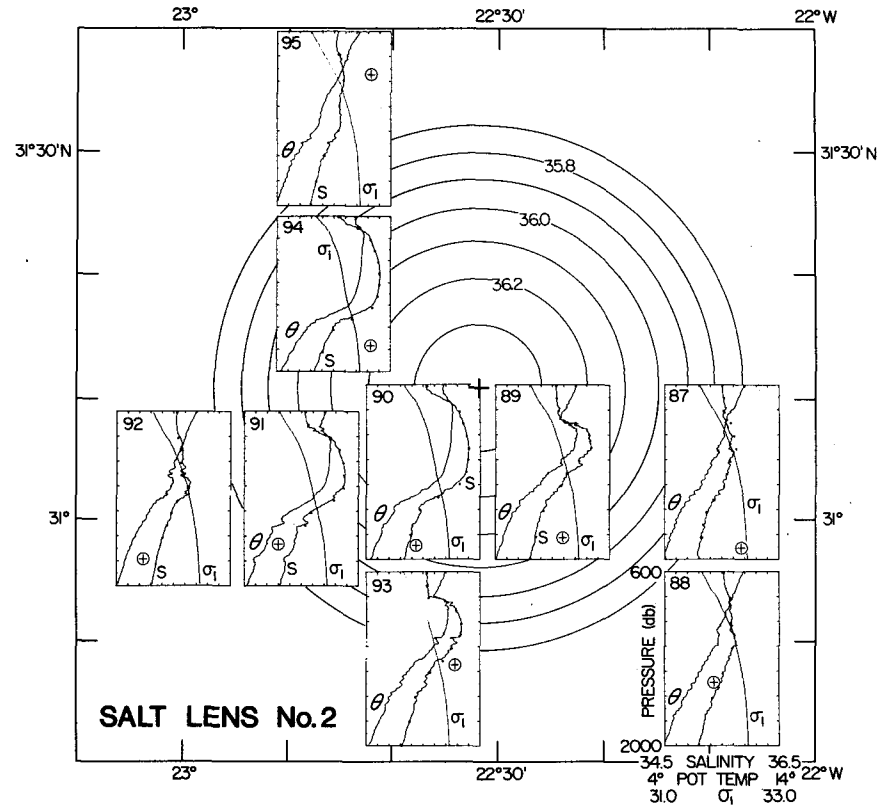

FIG. 12. As in Fig. 11 but for salt lens 2.

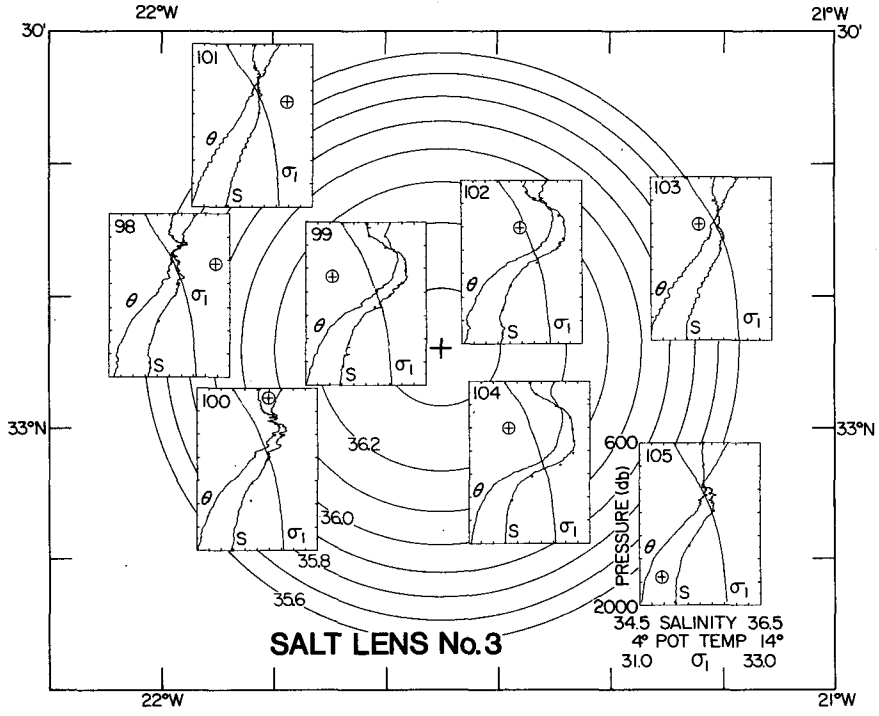

FIG. 13. As in Fig. 11 but for salt lens 3.

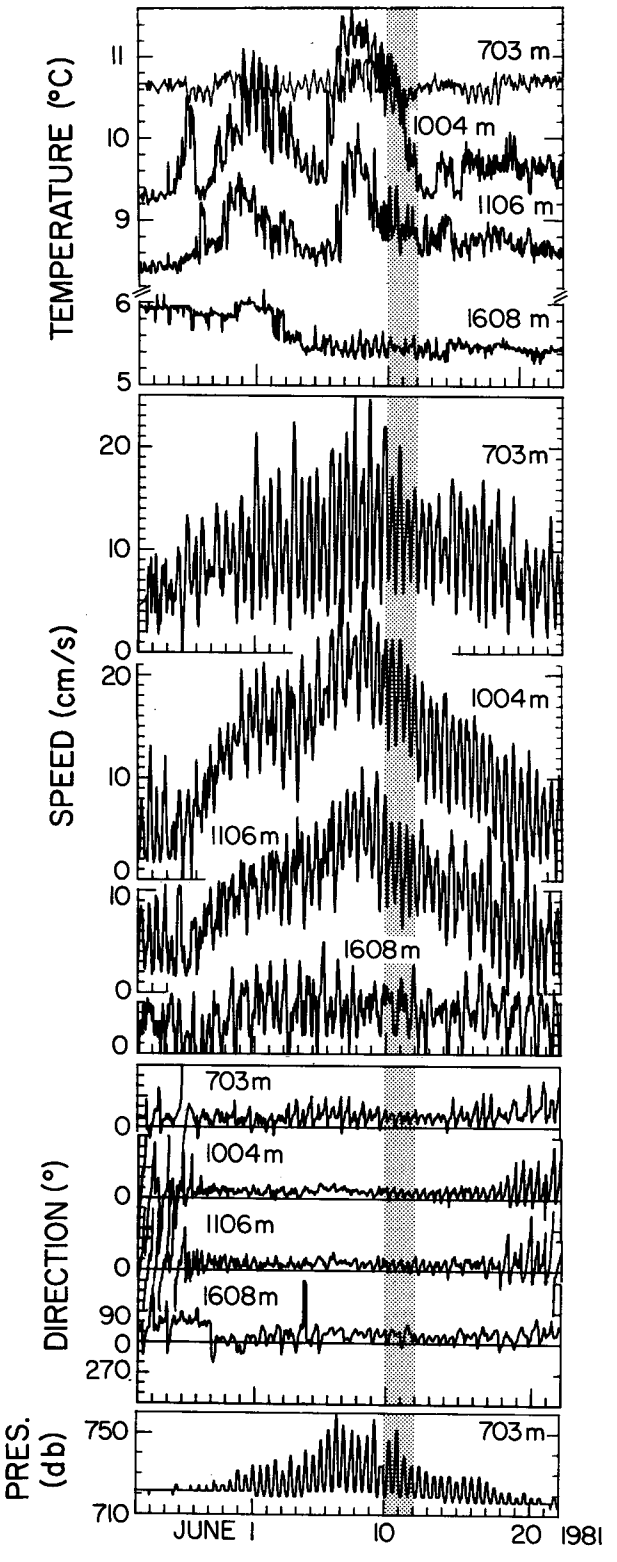

FIG. 14. Temperatures, speeds and directions at nominal depths of 703, 1004, 1106, 1608 m and pressure deviation at 703 m from Kiel mooring 276. (33°9.9'N, 21°50.9'W). The stippled time period (10–11 June 1981) represents the time frame of hydrographic observation of lens 3.

TABLE 2. Statistics of hourly sampled data from mooring site 276 (33°9.9'N, 21°50.9'W) between 24 May and 21 June 1981.

	IFM mooring number			
	276108	276109	276110	276111
Nominal depth	703 m	1004 m	1106 m	1608 m
Speed (cm s^{-1})				
Mean	9.8	12.6	9.7	3.9
Std. dev.	4.6	6.2	4.4	2.2
Max	24.8	29.0	22.1	11.0
Mean direction (°)	52	54	71	68
Pressure (db)				
Mean	724	—	—	—
Std. dev.	8.1	—	—	—
Temperature (°C)				
Mean	10.6	9.95	8.84	5.61
Std. dev.	0.12	0.60	0.33	0.21
Max	11.0	11.57	10.19	6.17
Min	10.25	9.18	8.35	5.28

tures during the 3 days at the beginning of the chosen subsample. The directions at these two levels are strongly variable. At 1106 m, 360 degree turns of the moderate speed O(10 cm s^{-1}) current, modulated by the semidiurnal period, can be seen. The pressure record shows a stable mooring. Around 27 May the temperature rises more than 1°C within a day at both 1004 and 1106 m. The temperature signal at 703 m is unaffected except for the characteristic semidiurnal tidal oscillation, seen in nearly all records at all depths from mooring 276. The direction stabilizes with tidal variations of less than 30°. Speeds at 1004 and 1106 m increase steadily and reach maxima of 29 and 22 cm s^{-1} on 8 June. Of further interest are the strong speed pulsations (up to 18 cm s^{-1} during a tidal cycle) at 703 m which are correlated with the pressure and temperature records from that level. Tidal fluctuations of speed O(10 cm s^{-1}) and pressure O(30 db) are in phase, speed and temperature O(0.3°C) are in counterphase. After the maximum speed occurred, speeds at the Mediterranean Water level decrease in a nearly symmetric way, compared to the increase, until 19 June when the current direction becomes less stable again. Since the direction of flow changes little during the period that lens 3 was observed at the mooring, we surmise that it didn't actually pass by the mooring. Instead, the lens appears to have moved in and then backed out again.

The hydrographic survey of lens 3 was conducted during the decreasing velocity period between 10 and 11 June. The 1608 m records do not indicate any evidence of salt lens 3. The uncorrelated temperature step on 2 June may indicate a water mass transition in the Deep Water. The departure of the lens after 19 June only seems to be characterized by more variability in direction at the 1608 m level.

4. Comparison with hydrography

The plots of potential temperature and dynamic height versus radius of Figs. 8–10 can be compared with the data from the current meters at Kiel mooring 276. At the time of the hydrographic observations (10–11 June), a velocity of 20–25 cm s^{-1} was seen at 1004 m with a direction of ~30°. This is the direction suggested also by the position of the current meter mooring shown in Fig. 7; the velocity has the correct magnitude as seen from the plot of dynamic height versus radius of Fig. 10. The direction of ~30° is also tangent to the isohaline at the position of the mooring. It should be noted that the temperature anomaly of greater than 2°C provides an excellent conditional sampling criterion for these velocity records.

Vertical shears are small over a large portion of the lens as can be inferred by the distribution of dynamic height gradients in Fig. 15. In the 400 db pressure interval from 800 db to 1200 db, dynamic height gradients changes and hence velocities shears are small, $\sim 0.2 \times 10^3$ s^{-1}. We do not yet know, of course, what the radial velocity distribution within a lens actually is, but if the distribution of properties is any indication, the center is well mixed. If momentum

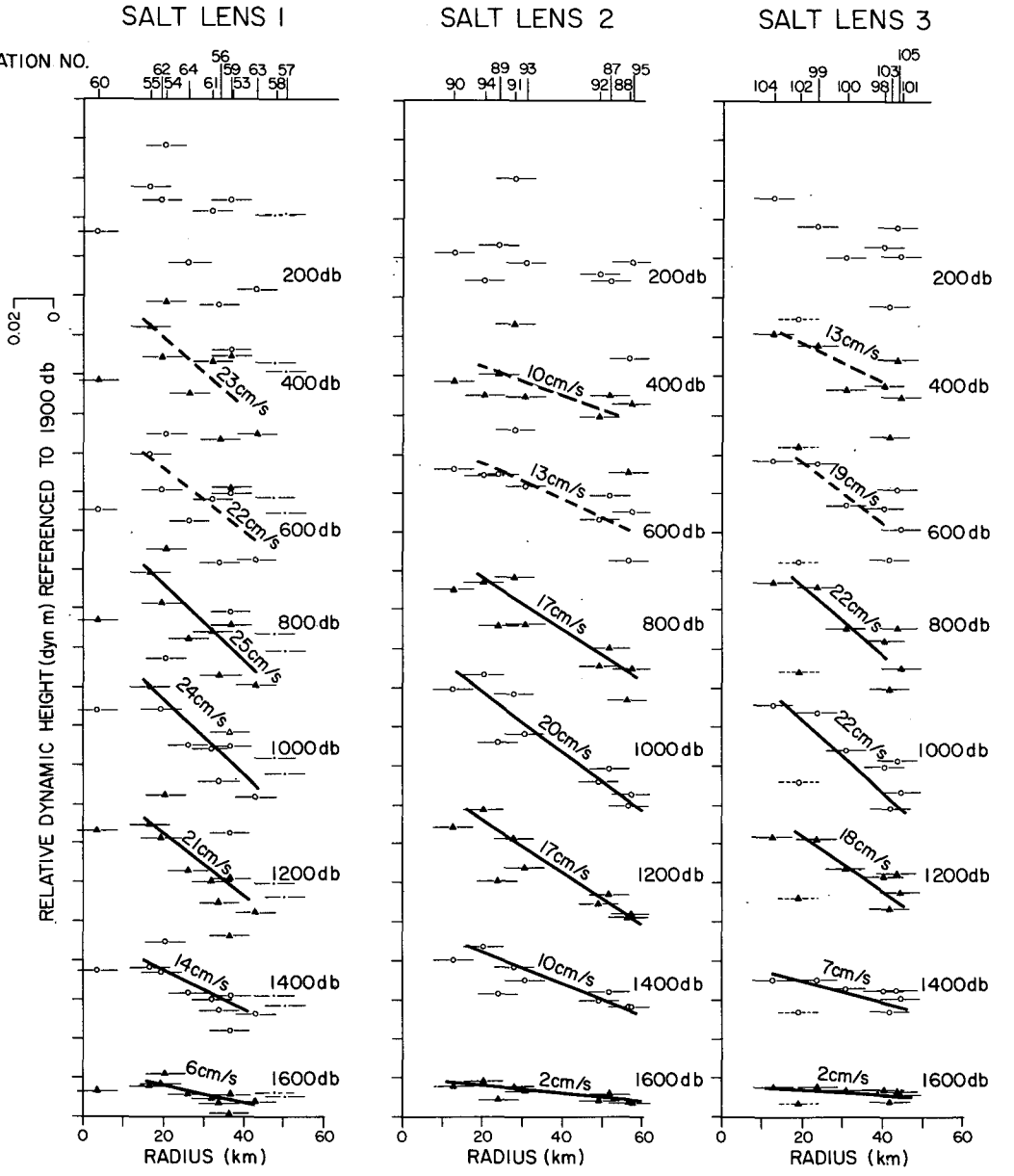

FIG. 15. Radial distributions of relative dynamic height at 200 db intervals. Salt lens 1–3.

mixed radially like a scalar (turbulent Schmidt number of unity), the center will rotate as a solid body. Velocity would then increase radially in the well-mixed center and then decay towards the edge of the lens. The dynamic height data (Fig. 15) are somewhat ambiguous, but they imply a broad maximum with the radial gradient going to zero at lens center. At the 400 and 600 db surfaces the dynamic height gradient is drawn as a dashed rather than solid line to emphasize the uncertainty in estimating the gradient above other fluctuations in dynamic height at these levels.

5. Long-term records

We now consider the long-term behavior of currents and temperatures in the depth interval of the Mediterranean Water at mooring 276. Tidal oscillations have been filtered, resulting in a time series with a sampling rate of 1 data point per day. With the replacement of mooring 2761 by 2762 (33°4.8'N, 21°53'W) in July 1981 we were able to compose a 16.5-month composite current meter record using the 1106 and 1160 m records for the first and second half respectively. Figure 16 shows the resultant time series of temperature and speed.

In the composite progressive vector (provec) diagram (Fig. 17) prevailing current directions can be seen. Added to Fig. 17 is the provec diagram for the time series at 1004 m depth, available only for the first half of the composite series. This provec has been shifted (without turning) in such a way that time marks at the time of maximum speed (8 June 1981) are adjacent to the provec at 1106 m. The deviation of the lines in Fig. 17, connecting every 5-day tic mark, indicates vertical shear within lens 3. While in general the shear seems remarkably low, during passage of the lens there is an increase of the low-passed shear to $\sim 0.4 \times 10^{-3}$ s^{-1}.

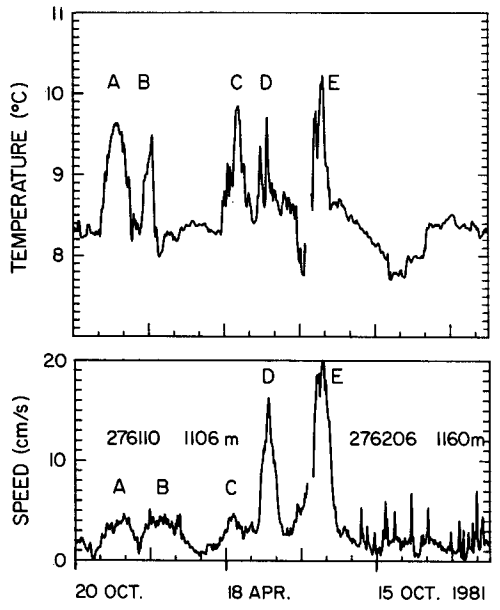

FIG. 16. Low-passed composite temperature and speed time series from mooring 276 at 1106 and 1160 m. Periods labeled A–E show correlated temperature speed increases. Period D is shown in detail in Fig. 14.

Apparently no "mean" current vector can be determined from the composite record. Obviously the meridional component dominates also the Mediterranean water level as discussed by Käse *et al.* (1984) for the upper thermocline, the Warmwassersphäre. However, virtually all water displacements with anomalously high temperatures appear to be periods with a strong meridional component. We have labeled the five high temperature periods by letters A–E. This notation was reproduced from the low-passed time series, Fig. 16. Period D has already been treated in detail (cf. the subsample in Fig. 12). In describing all high temperature periods, which happened only during the first ⅔ of the record, we note that they are all of the same order of magnitude. This is not the case in the corresponding speed series. There we can distinguish between low speed (A–C) and high speed (D–C) events. The classification into two groups, the low and the high energetic anomalies, can be seen more clearly in Fig. 18. In this scatter diagram of the composite series we also have included data from the 1004 m level. Independent studies from R.V. *Poseidon* in April 1982 have revealed that the strongest of all events E could be traced through the whole thermocline up to the surface (Käse and Rathlev, 1982). Käse and Siedler (1982) have associated this with the meandering of the subtropical front in the Canary Basin.

Events in the speed series are certainly longer in duration than their associated temperature anomalies which were already mentioned in the lens study, period D. From the longer duration of the speed anomaly one might conclude that part of the eddy spin has transferred into the surrounding colder, less saline background water mass. Although we have no further evidence for this discrepancy, we note that it must have substantial impact on the dynamics of the whole salt-lens phenomenon, including mixing and fine structure distributions (cf. Figs. 11–13) at the boundaries of the lenses.

Although we can distinguish between low- and high-energetic speed anomalies in our long-term series, we are unable with data from a single point mooring to relate this classification to possibly different physical processes such as water mass fronts and lenses within the Mediterranean Water. Only in period D (lens 3) do we have hydrographic data for the salt lens. In case E we do know that there existed a direct relationship to the subtropical front covering the whole

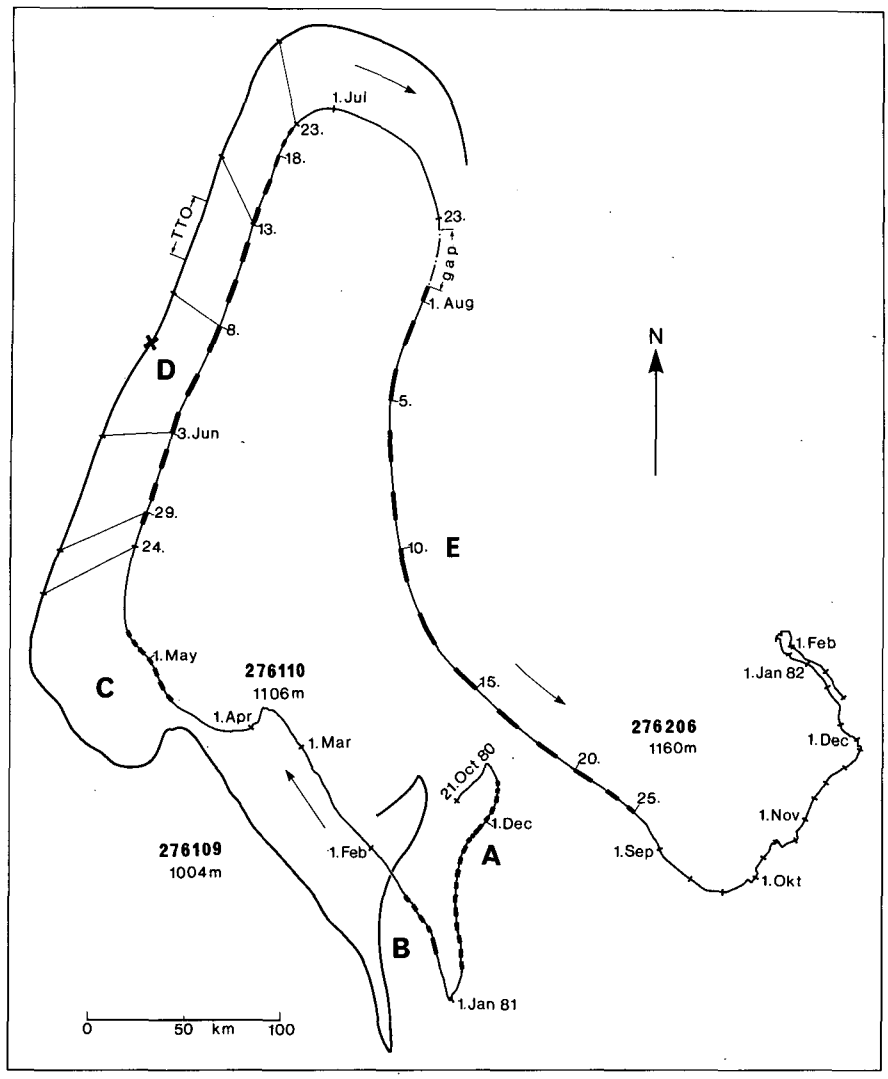

FIG. 17. 16.5-month progressive vector diagram for mooring 276. The semi-continuous curve represents virtual water displacements at (1106, 1160) m depth during its (first, second) half. The gap was caused by mooring replacement and data loss due to low-pass filtering. Periods with high temperature anomalies (cf. Fig. 17) are labeled A–E. The additional curve from 1004 m has been shifted (without turning) in such a way that time marks from the maximum speed occurrence (8 June 1981) are next to each other. The X during period D is at the time of maximum mooring depression shown in Fig. 14. The survey period is labeled TTO.

Warmwassersphäre; its interaction with the Mediterranean Water is not yet understood.

6. Origin, probability and ages

The salinity and silicate field at $\sigma_1 = 32.2(\sigma_\theta \sim 27.7)$[2], are shown in Figures 19 and 20 for the data collected on R.V. *Knorr*. The corresponding pressure field is shown in Fig. 21. Figure 19 clearly shows the importance of the lenses to understanding the background signature of the more diffuse traditional Mediterranean salt tongue also shown on the figure. Although we do not yet know about the dynamics and evolution of the lenses, they clearly represent a sizable signal compared to that of the tongue itself. The silicate field is completely conjugate to the salinity field, as is to be expected for a Mediterranean source. In contrast, the oxygen field (Fig. 22) shows no anomalies associated with the lenses or the Mediterranean tongue itself since the Mediterranean is not an anomalous source of oxygen.

In Table 3 properties at $\sigma_1 = 32.2$ near lens centers

[2] The conversion from $\sigma_1 = 32.2$ is only approximate. At the lens centers $\sigma_\theta = 27.75(S \sim 36.2)$ whereas for a background station $\sigma_\theta = 27.70(S \sim 35.5)$.

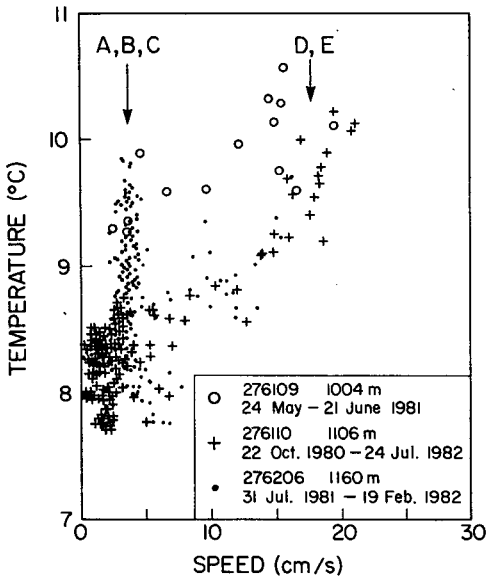

FIG. 18. Scatter plot showing temperature-speed dependence. Refer to the time series (Fig. 17) for event annotation of periods A–E.

(stations 60, 90, 104) can be compared with those of a typical nearby background station (85) as well as stations from the next leg (IV) of the TTO expedition (stations 110, 111, 112 and 113). Station positions are also shown in Fig. 2. The lens stations have properties most like those found at station 113 just to the north of Cape St. Vincent, Portugal ~ 1000 km away. Water mass characteristics of the lenses are also similar to those found in the near outflow described by Ambar *et al.* (1976). A deep eddy off Cape St. Vincent was found by Swallow (1969). However this eddy was cyclonic, in direct contrast to the three anticyclonic eddies reported on here. Arguments have also been given by Zantopp and Leaman (1982) for a Gulf of Cadiz origin for a thermocline eddy observed in the Western North Atlantic.

Previous work of Zenk (1971, 1975a,b) has treated the outflow primarily east of 15°W where he could find no evidence for salt lenses or eddies. Recent analysis by Gründlingh (1981) has shown a solitary event of 2–4 days duration due to thickening of the Mediterranean Overflow and an increase in the volume transport.

It is possible to speculate on how often a salt lens is formed based on the estimates of Zenk (1975a, Fig. 9) for volume flow of the Mediterranean outflow. After some dilution with North Atlantic Water to a salinity of ~36.5, the main flow is $\sim 1.4 \times 10^6$ m^3 s^{-1} (1.4 Sv) whereas the total flow, including all branches, is $\sim 2.9 \times 10^6$ m^3 s^{-1} (2.9 Sv). With the

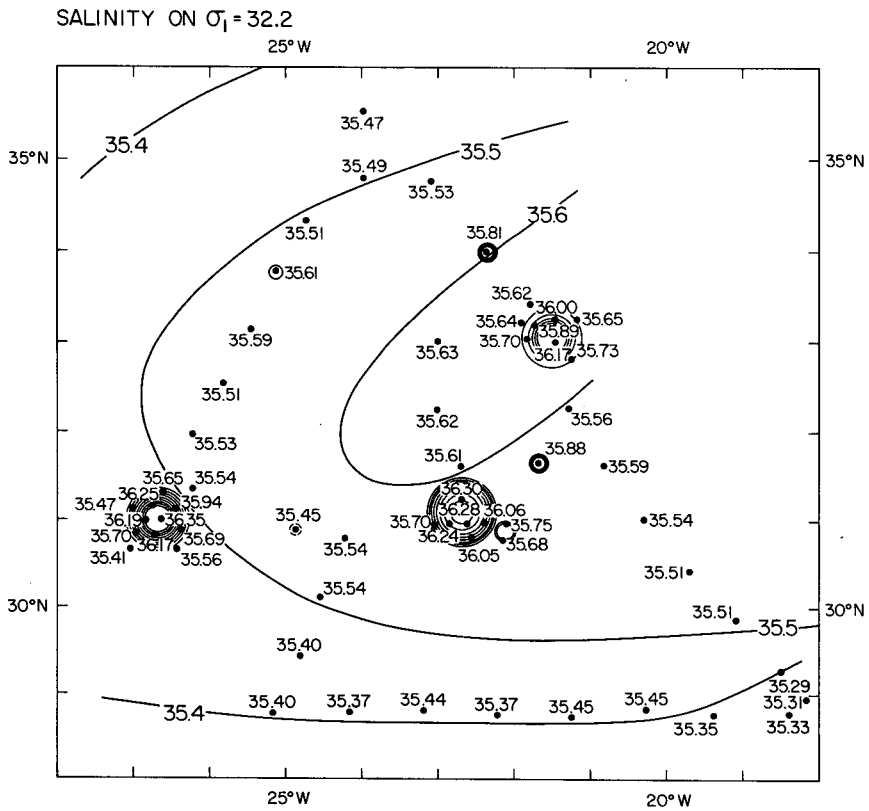

FIG. 19. The salinity field at σ_1 = 32.2($\sigma_\theta \sim$ 27.7) during June 1981 in the Canary Basin. The contour interval is 0.1. The salt lenses and fluctuations of the background field are all contoured. Positive anomalies are shown with solid circles; negative anomalies are dashed.

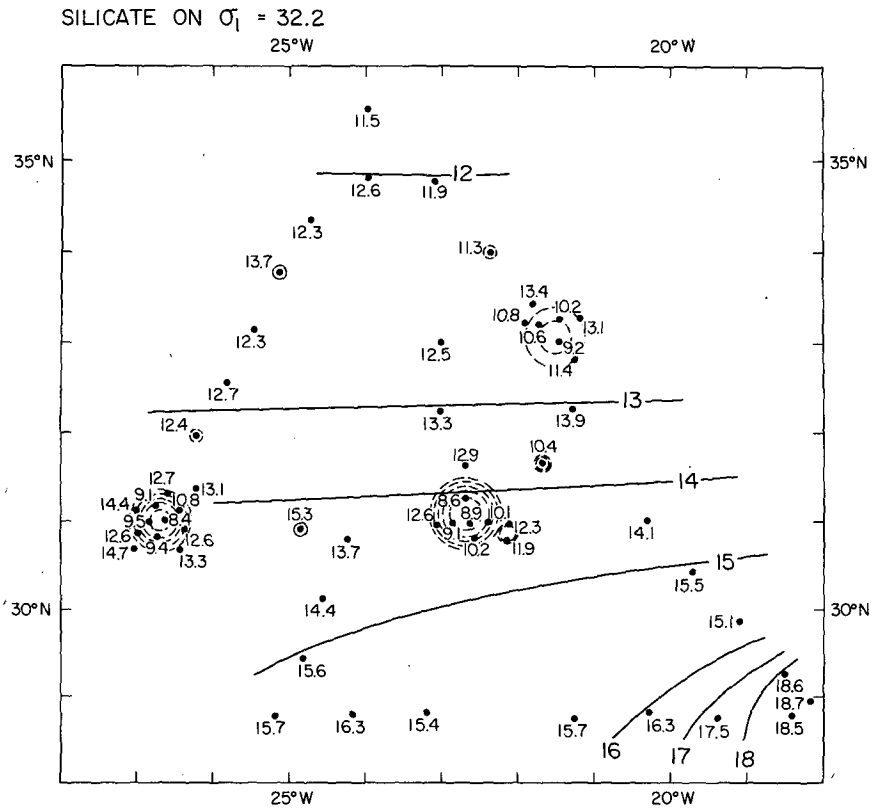

FIG. 20. The silicate field (μm kg^{-1}) at σ_1 = 32.2($\sigma_\theta \sim$ 27.7) during June 1981 in the Canary Basin. The background and anomalies are all contoured in the same way. Note that negative anomalies of silicate coincide with positive salinity anomalies of Fig. 20.

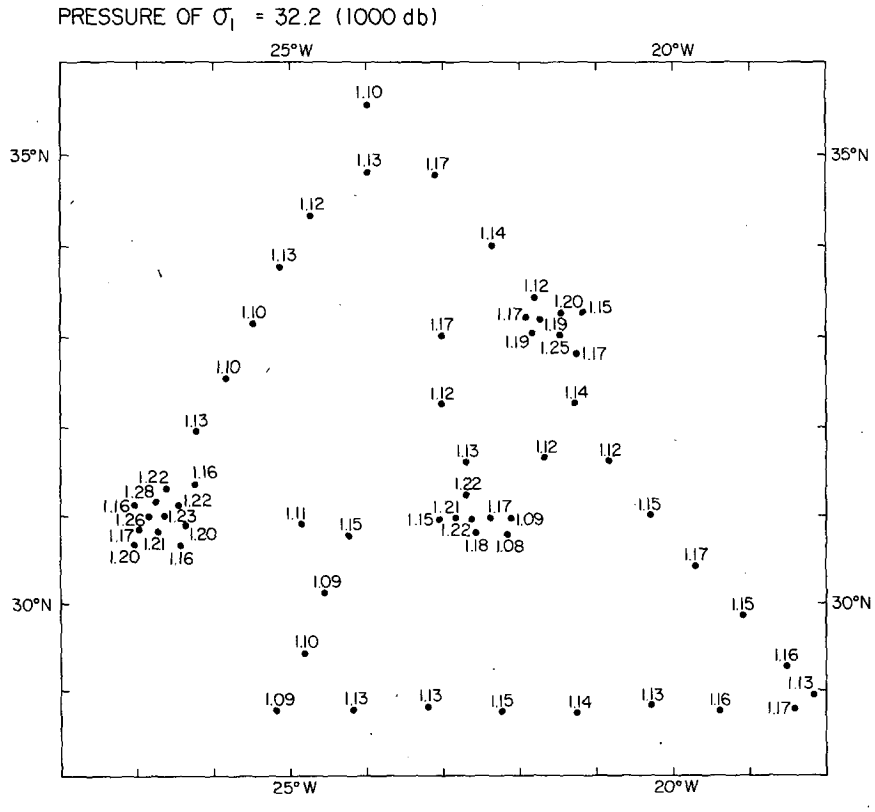

FIG. 21. The pressure (1000 db) of the σ_1 = 32.2($\sigma_\theta \sim$ 27.7) surface during 1981 in the Canary Basin.

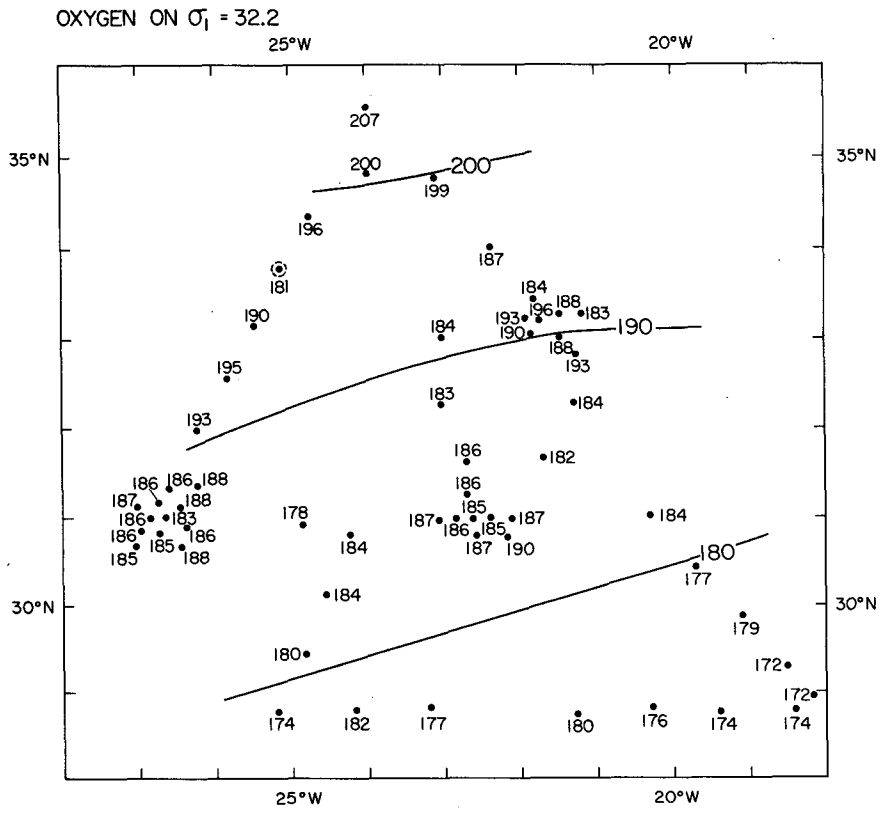

FIG. 22. Oxygen concentration (μm kg^{-1}) at σ_1 = 32.2($\sigma_\theta \sim$ 27.7) during the June 1981 in the Canary Basin. Note the salt lenses have no anomalous oxygen concentrations.

main flow alone ~20 days are needed to form a salt lens of the size found in the Canary Basin, whereas with the total flow only ~10 days are needed.

Ages of these lenses are difficult to estimate. Although transient tracers were collected, their interpretation awaits a better characterization of the Mediterranean Outflow source. Based on the distance (~1000 km) from the outflow and mean advection speeds of say 1–3 cm s^{-1}, 1–3 years would be appropriate ages. Lenses are apparently long lived. Observations which could be interpreted as lenses to the east of the Canary Basin (25°W) have been made by Armi and Stommel (1983), McDowell and Rossby (1978), Rossby *et al.* (1983) and Riser *et al.* (1984). With the exception of the single station reported by Armi and Stommel, none of these observations shows the strong property anomalies found here, indicating decay by as yet unknown processes.

The probability of actually finding lenses in the Canary Basin is high. Along the station track of TTO Leg III (Fig. 2) at a station spacing of ~80 km, 3 lenses were found among 36 independent stations (excluding all the stations devoted to detail surveying of each lens). This gives a probability of ~0.08 of finding a lens at any location in the Canary Basin. If the statistics of area covered by lenses were calculated

TABLE 3. Interpolated values of salinity, silicate, pressure, and oxygen at σ_1 = 32.2($\sigma_\theta \sim$ 27.7).

Station	Salinity	Silicate (μm kg^{-1})	Pressure (1000 db)	Oxygen (μm kg^{-1})	Position
85	35.56	13.9	1.14	184	32°16′N, 21°17′W
60 (lens 1)	36.35	8.4	1.23	183	31°0′N, 26°39′W
90 (lens 2)	36.28	8.9	1.22	185	30°50′N, 22°38′W
104 (lens 3)	36.17	9.2	1.25	188	33°0′N, 21°28′W
110	35.45	11.9	1.10	206	37°35′N, 22°40′W
111	35.85	11.3	1.11	187	37°53′N, 17°28′W
112	36.12	9.9	1.07	186	37°36′N, 13°29′W
113	36.28	9.2	1.08	186	37°35′N, 10°20′W

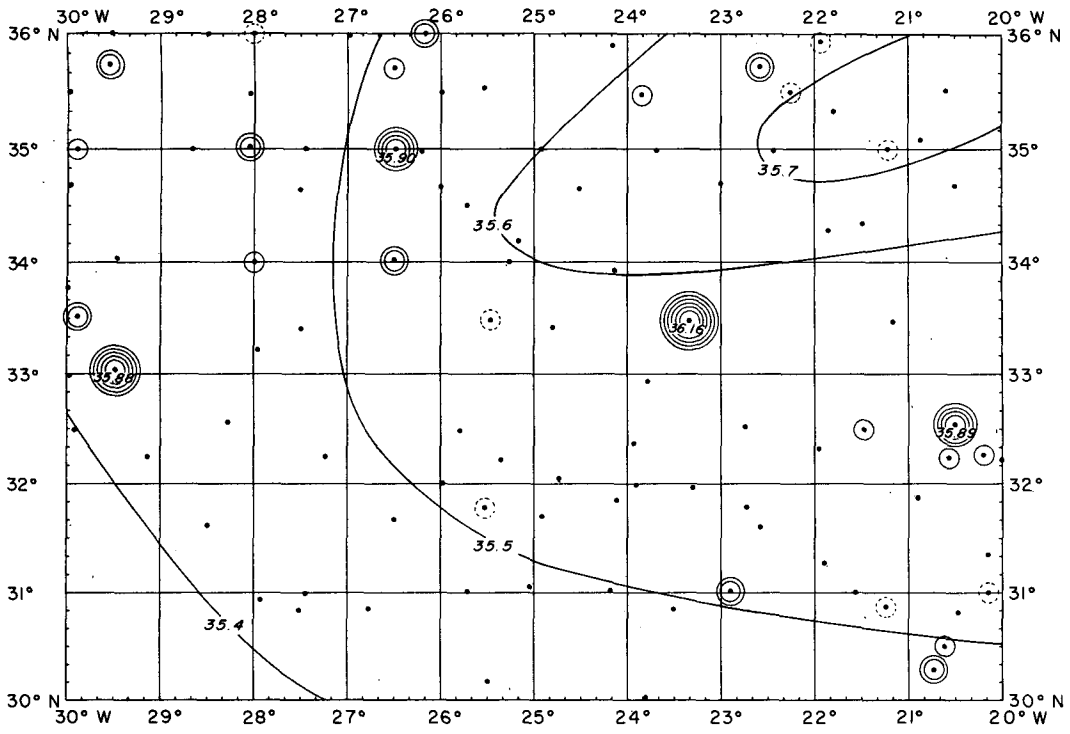

FIG. 23. Salinity on $\sigma_1 = 32.2(\sigma_\theta \sim 27.7)$ surface—NODC historical data up to 1972.

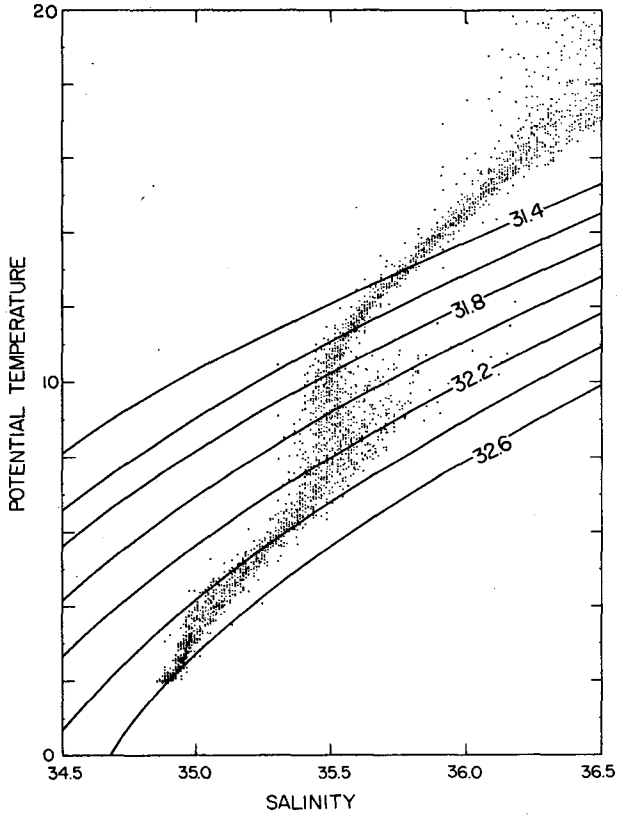

FIG. 24. Potential temperature vs. salinity—NODC historical data up to 1972. σ_1 lines are shown for reference.

on the basis of the temperature record shown in Fig. 16 from a single site mooring, the probability would be over .2.

The archival NODC data are displayed in Fig. 23 as salinity at $\sigma_1 = 32.2$. Only selected stations with reliable deep-water potential temperature and salinity (θ, S) characteristics were retained as shown in Fig. 24. The data retained were taken between 1914 and 1972. Figure 23 should be compared with Fig. 19 which shows similar data taken only in June 1981. Although none of the lenses is resolved by the individual stations from the NODC archive, the distribution of anomalies along the Mediterranean salt tongue is similar in Figs. 19 and 23. It is somewhat mysterious as to why these anomalies had not been recognized before.

Traditionally tongues of various properties in the ocean have been interpreted as due to an advective–diffusive balance from a source. Examples of such interpretations for the Mediterranean Water are the work of Defant (1955), Needler and Heath (1975), Richardson and Mooney (1975), Armi and Haidvogel (1982) and Armi and Stommel (1983). Armi and Haidvogel, as well as Armi and Stommel, recognized that the existence of salt lenses casts serious doubt on gradient transport process. It was suggested that if salt lenses are associated with a significant transport of Mediterranean water and are not just an occasional event, then a model for tongue-like property distributions need be adopted which includes these lenses.

The simplest way to treat them within an existing steady state framework would be as a distributed source. Each lens presumably travels to a different location before breaking apart. Hence the Mediterranean outflow does not really inject salty water at the coast alone but may be thought of as a source distributed in some as yet unknown way beginning at the outflow and extending into the basin at least 2000 km.

Armi and Stommel (1983) estimated that only three lenses per year need enter and break apart in their triangle in order to have a flux divergence equal to the advective flux divergence. For the area of study here at the edge of the subtropical gyre (cf. Käse and Siedler, 1982) it is difficult actually to estimate from the weak dynamic height gradients a meaningful advective flux divergence at the level of the salt lenses. The existence of at least the three lenses surveyed suggests that a sizable contribution to, if not most, of the flux divergence of salt is due to this distributed source.

7. Summary and conclusions

Isolated compact anticyclonic eddies or salt lenses appear to be a fairly common phenomenon of the Canary Basin. Hydrographic/CTD surveys of three such lenses show them to be centered at a depth of ~1100 m. Their anomalies of salinity and temperature are large (~0.8, 2.5°C) as are their vertical extent at center (~900 m). Although as yet poorly resolved, their radial structure is not badly represented as axisymmetric and lens-like with typical radii of ~50 km. Current meter records indicate anticyclonic velocities of up to 29 cm s^{-1}. The probability of finding a salt lens at any station in the Canary Basin is fairly high (~0.08). Fine structure with vertical scales ~20 m and less, possibly due to intrusive decay, appears at the outer edges of the lenses. In contrast, stations near the lens centers appear free of fine structure and relatively smooth.

Typical Väisälä frequencies near lens center can be as low as ~1.2 cph, whereas background values are typically ~1.6 cph. We do not, however, believe we are able to resolve the radial structure of the lenses well enough for comparison with models proposed (cf. Nof, 1981; Dugan *et al.*, 1982; Ikeda, 1982; Killworth, 1983; and McWilliams, 1984). Unfortunately one aspect of models with homogeneous lenses is that velocity increases radially (cf. Dugan *et al.*, 1982), whereas the observed velocities appear to increase radially in a near solid body-like center and then decrease radially to the lens edge. (See also Riser *et al.*, 1984.) Stratified models of the type proposed by McWilliams (1984) seem more appropriate, given the observed horizontal and vertical gradients of water properties (S, θ, silicate), Väisälä frequency (N) and velocity.

Acknowledgments. It is with pleasure that we acknowledge the assistance of Sharon Yamasaki with programming and data analysis. The hydrographic data were collected by the SIO Physical and Chemical Oceanographic Data Facility (PACODF) as part of the Transient Tracers in the Oceans (TTO) North Atlantic Study. Our research is funded by the National Science Foundation and Office of Naval Research (L.A.) and by the Deutsche Forschungsgemeinshaft, Bonn (W.Z.).

REFERENCES

Ambar, I., M. R. Howe and M. I. Abdullah, 1976: A physical and chemical description of the Mediterranean outflow in the Gulf of Cádiz, *D. Hydrogr. Z.* **29,** 58–68.

Armi, L., 1978. Some evidence for boundary mixing in the deep ocean. *J. Geophys. Res.*, **83,** 1971–1979.

——, 1981: Large lenses of highly saline Mediterranean Water. Eos, **62,** 45, 935. [Abstract 05-1-C-14]

——, and E. D'Asaro. 1980. Flow structures of the benthic ocean. *J. Geophys. Res.*, **85,** 469–484.

——, and D. B. Haidvogel, 1982: Effects of variable and anisotropic diffusivities in a steady state diffusion model. *J. Phys. Oceanogr.*, **12,** 785–794.

——, and H. Stommel, 1983: Four views of a portion of the North Atlantic Subtropical Gyre, *J. Phys. Oceanogr.*, **13,** 828–857.

Defant, A., 1955: Die Ausbreitung des Mittelmeerwassers im Nordatlantischen Ozean. *Pap. Mar. Biol. Oceanogr.*, Deep Sea Res., **3**(Suppl), 465–470.

Dugan, J. P., R. P. Mied, P. C. Mignerey and A. F. Schuetz. 1982: Compact, intra-thermocline eddies in the Sargasso Sea. *J. Geophys. Res.*, **87,** 385–393.

Gründlingh, M., 1981: On the observation of a solitary event in the Mediterranean Outflow west of Gibraltar. *Meteor Forsch. Ergenbn.*, **A/B23,** 15–46.

Ikeda, M., 1982: A simple model of subsurface mesoscale eddies. *J. Geophys. Res.*, **87,** 7925–7931.

JPOTS, Joint Panel on Oceanographic Tables and Standards, UNESCO/ICES/SCOR/IAPSO, 1980: Background papers and supporting data on the international equation of state of sea water. UNESCO Tech. Pap. in Mar. Sci., **38,** 192 pp.

Käse, R., and J. Rathlev, 1982: CTD data from the North Canary Basin. Poseidon cruise 86/2, 26 March–13 April 1982. Ber. Inst. f. Meeresk. Kiel/103.

——, and G. Siedler, 1982: Meandering of the subtropical front south-east of the Azores. *Nature,* **300,** 5889, 245–246.

——, W. Zenk, T. B. Sanford and W. Hiller, 1984: Currents fronts, and eddy fluxes in the Canary Basin. *Progress in Oceanography,* Pergamon, (in press).

Killworth, P. D., 1983: On the motion of isolated lenses on a beta-plane. *J. Phys. Oceanogr.*, **13,** 368–376.

McDowell, S. E., and H. T. Rossby, 1978: Mediterranean water: An intense mesoscale eddy off the Bahamas. *Science,* **202,** 1085–1087.

McIntyre, M. E., 1970: Diffusive destabilization of the baroclinic circular vortex. *Geophys. Fluid Dyn.*, **1,** 19–58.

McWilliams, J. C., 1984: Sub-mesoscale, coherent vorticies in the ocean. Submitted to *J. Phys. Oceanogr.*

Müller, T. J., 1981: Current and temperature measurements in the North–East Atlantic during NEADS. Ber. Inst. f. Meeresk. Kiel/90, 100 pp.

——, and W. Zenk, 1983: Some Eulerian velocity observations and XBT sections from the North East Atlantic, October 1980–July 1982. Ber. Inst. f. Meeres. Kiel/Nr. 114, 145 pp.

Needler, G. T., and R. A. Heath, 1975: Diffusion coefficients calculated from the Mediterranean salinity anomaly in the North Atlantic Ocean. *J. Phys. Oceanogr.*, **5,** 173–182.

Nof, D., 1981: On the movement of deep mesoscale eddies in the North Atlantic. *J. Mar. Res.*, **40,** 57–74.

Physical and Chemical Oceanography Data Facility, 1981: Transient Tracers in the Ocean Preliminary Hydrographic Report Leg 3. PACODF Publ. No. 215, Scripps Institution of Oceanography, La Jolla, CA, 268 pp.

Piip, A. T., 1969: Large cells of Mediterranean water in the Madeira-Canaries region. Eos, 50, 193. [Abstract 068.]

Richardson, P. L., and K. Mooney, 1975. The Mediterranean Outflow-a simple advection-diffusion model. *J. Phys. Oceanogr.*, **5,** 476–482.

Riser, S. C., W. B. Owens, H. T. Rossby and C. C. Ebbesmeyer, 1984: The structure, dynamics, and origin of a small-scale lens of water in the Western North Atlantic Thermocline. Submitted to *J. Phys. Oceanogr.*

Rossby, H. T., S. C. Riser and A. J. Mariano, 1983: The Western North Atlantic—A Lagrangian viewpoint. *Eddies in Marine Science,* A. R. Robinson, Ed., Springer, 609 pp.

Siedler, G., and W. Zenk, 1973: Variability of the thermohaline staircase. *Nature,* **244,** 11–12.

Swallow, J. C., 1969: A deep eddy off Cape St. Vincent. *Deep Sea Res.,* **16**(Suppl.), 285–295.

Turner, J. S., 1973: *Buoyancy Effects in Fluids.* Cambridge University Press, 367 pp.

Uchupi, L., 1971: *Bathymetric Atlas of the Atlantic, Caribbean, and Gulf of Mexico,* Ref 71–72. Woods Hole Oceanographic Institution, Woods Hole, MA 02543.

Zantopp, R., and K. Leaman, 1982: Gulf of Cadiz water observed in a thermocline eddy in the Western North Atlantic. *J. Geophys. Res.,* **87,** 1927–1934.

Zenk, W., 1971. Zur Schichtung des Mittelmeerwassers westlich von Gibraltar. *Meteor Forsch. Ergenbn.,* **A9,** 1–30.

——, 1975a. On the Mediterranean outflow west of Gibraltar. *Meteor Forsch. Ergebn.,* **A16,** 23–34.

——, 1975b. On the origin of intermediate double maxima in T/S Profiles from the North Atlantic. *Meteor Forsch. Ergebn.,* **A16,** 35–43.